Acta Chemica Scandinavica, 1995: 49: 85–95
Printed in Belgium – all rights reserved

ACTA
CHEMICA SCANDINAVICA
ISSN 0904-213X

Chemistry of Niobium Chlorides in the CsCl–NaCl Eutectic Melt. 2. Voltammetric Studies of Niobium Chlorides and Oxochlorides in the CsCl–NaCl Eutectic Melt

Christian Rosenkilde and Terje Østvold†

Institute of Inorganic Chemistry, The Norwegian Institute of Technology, N-7034 Trondheim, Norway

Rosenkilde, C. and Østvold, T., 1995. Chemistry of Niobium Chlorides in the CsCl–NaCl Eutectic Melt. 2. Voltammetric Studies of Niobium Chlorides and Oxochlorides in the CsCl–NaCl Eutectic Melt. – Acta Chem. Scand. 49: 85–95

Cyclic voltammetry has been used to study the reduction mechanisms of niobium chlorides and oxochlorides in the CsCl–NaCl eutectic melt at temperatures between 823 and 973 K. Nb(V) in the melt is reduced in two steps to Nb(III): $NbCl_6^- + e^- = NbCl_6^{2-}$ with $E_{1/2} = -0.31$ V versus the standard chlorine electrode, and $NbCl_6^{2-} + e^- = NbCl_x^{(x-3)-} + (6-x)Cl^-$, ($x = 4$, 5 or 6), with $E_{1/2} = -1.14$ V. $NbCl_x^{(x-3)-}$ is reduced to the metal in several unidentified steps occurring at potentials from −1.6 to −2.0 V. In oxide-containing melts $NbOCl_5^{2-}$ ions are reduced in two steps: $NbOCl_5^{2-} + e^- = NbOCl_x^{(x-2)-} + (5-x)Cl$, ($x = 3$, 4 or 5) with $E_{1/2} = -1.19$ V and $NbOCl_x^{(x-2)-}$ to a solid, probably NbO(s) at −1.8 V. $NbO_2Cl_x^{(x-1)-}$ ($x = 3$ or 4) ions probably also exist in $NbCl_5$-containing melts saturated with Nb_2O_5. This ion is probably reduced to NbO_2(s) at −1.39 V. In melts containing Cs_2NbOCl_5, Nb_2O_5(s) and Nb metal, Nb(IV) oxochlorides with a molar ratio O/Nb = 1 are the main niobium-containing ions in the solution. These ions may oxidise to $NbOCl_5^{2-}$, and when reduced a solid, probably NbO(s), at about −1.6 V is formed. Moreover, Nb(IV) oxochloride ions react with glassy carbon, forming niobium carbide. The electrodeposition of niobium on steel has also been studied, and to obtain pure, dense and coherent niobium metal deposits it is important to establish equilibrium between the niobium-containing ions in solution and niobium metal. Moreover, the temperature during deposition should be higher than about 920 K. In melts where O/Nb ≥ 1, metallic deposits were not obtained.

Previously, Raman spectroscopic studies[1] in the system $CsCl$–$NbCl_5$–$NbOCl_3$, absorption spectroscopic studies[2] of niobium chlorides and oxochlorides in molten alkali chloride melts, and EMF measurements[3] of $NbCl_3$ in the CsCl–NaCl eutectic melt have been presented. In this paper we focus on the reduction mechanism of niobium chlorides and oxochlorides in the CsCl–NaCl eutectic melt. Mellors and Senderoff,[4] using an alkali fluoride melt, were the first to report successful electrodeposition of niobium on steel. A number of other investigations on the electrochemistry of niobium in both alkali fluoride, alkali chloride and mixed chloride fluoride melts have also been presented[5–21] throughout the last three decades. So far, high-quality electrodeposits of niobium on steel from alkali chloride melts have not been reported. However, from both an economical and environmental point of view, such melts are better solvents for the deposition process than alkali fluoride melts. Moreover, in spite of the amount of results reported, there is still disagreement concerning the reduction mechanism of niobium chlorides. We therefore feel that it is worthwhile to study these matters further. Mellors and Senderoff[4] concluded that melts used for the electrodeposition of high-quality niobium deposits should be free from oxides. However, recently Christensen *et al.*[18] found that a small amount of oxide in LiF–NaF-KF eutectic melts containing niobium ions in equilibrium with niobium metal improved the current efficiency of the deposition reaction. Only a few studies on the electrochemistry of niobium oxochlorides have been published,[15,22] and the results of these studies do not agree. Because the influence of oxide ions on the deposition process of niobium seems to be important, and since there are some discrepancies in the previous work reported in this area, we have also investigated the reduction mechanism of niobium oxochlorides in alkali chloride melts.

† To whom correspondence should be addressed.

Experimental

Chemicals and equipment. Since niobium chlorides have a very high affinity for O^{2-} ions in melts, a base melt practically free from oxides was needed for our investigations. The experiments and handling of the purified salts were therefore carried out in a glove box with water content < 1 ppm and oxygen content < 5 ppm. A sample of the pure CsCl–NaCl eutectic melt was analysed as previously described.[3] The oxide content in the eutectic was below 10^{-6} mol%. The chemicals used and purification procedures are given in Table 1. $NbOCl_3$ was added as Cs_2NbOCl_5.[1] To obtain a 0.5 mol% $NbOCl_3$ solution, 0.8549 g Cs_2NbOCl_5 was added to 40.00 g of the CsCl–NaCl eutectic. To saturate the melt with Nb_2O_5, 0.650 g Nb_2O_5 was added. Finally, to study the reduced niobium oxochlorides, 2.20 g niobium metal were added.

The electrochemical cell has been described previously.[3] However, room for an additional electrode was provided in the cell. The reference electrode was a mullite tube closed in one end (∅ 10 × 6 mm Morgan Impervious Mullite, UK) with a silver wire dipping into a CsCl–NaCl eutectic melt containing 5 mol% AgCl.[3] Since oxide-free melts containing niobium in valence states five and four can dissolve both Al_2O_3 and SiO_2,[2,22–24] the reference electrode was dipped into the melt only during the voltammetric measurements. The reference electrode was raised above the melt when it was not in use, and no signs of corrosion on the electrode could be observed after the experiments. The working and counter-electrodes were glassy carbon rods (Carbone V25, 3 × 70 mm) connected to nickel rods by graphite connection pieces. The crucible was also made of glassy carbon (Carbone V25, ∅ 45 mm). The temperature was measured with a calibrated thermocouple (Pt/Pt, 10% Rh). Since Nb(V) chloride melts are known to oxidise gold,[25] and therefore probably also platinum, the wires of the thermocouple were only immersed into the melt for the time needed to read the stable temperature and were lifted well above the melt between measurements. A PAR M273A Potentiostat/Galvanostat was used to record the voltammograms. IR compensation was always employed to assure correct potential readings.

Table 1. Producers and purification procedures of the chemicals used.

Chemical	Producer and purification
CsCl	Fluka > 99.9%, dried with HCl and recrystallised
NaCl	Merck p.a., recrystallised
$NbCl_5$	Alfa grade 1, resublimed under vacuum
Nb_2O_5	Alfa 88291 > 99.9%, dried under vacuum
$NbCl_3$	Made from sublimed $NbCl_5$ (Alfa grade 1) and Nb (Alfa > 99.9%), according to Schäfer and Dohmann[23]
Nb	Alfa > 99.9%
AgCl	Fluka > 99%, dried under vacuum at 420 K

Electrodeposition experiments were performed in the same cell, but with a stainless-steel rod replacing the working electrode. In experiments where equilibrium between the dissolved niobium chlorides and niobium metal was established, a niobium metal rod was used as an anode. Otherwise, the glassy carbon counter-electrode was used. In the latter cases, care was taken not to deplete the melt of the niobium-containing species, and relatively low charges were transferred. Platinum, fused silica or glassy carbon crucibles were used in various deposition experiments. The depositions were performed galvanostatically, and a reference electrode was not employed. The stainless steel substrates were cleaned in nitric acid and dried before use. The furnace used was a Kanthal wound vertical and tubular furnace controlled with an Eurotherm controller. The furnace was mounted under the glove box in such a way that the experimental cell could be handled from inside the box. The temperature in the cell was stable within ± 2 K.

Modelling. The LSV models used in this work are based on the discreet point method described by Britz[26] and a third-order Runge–Kutta integration to solve the diffusion equations. To allow modelling of voltammograms with low sweep rates under limiting current conditions, a maximum Nernst diffusion layer has been introduced, defined by the equation

$$\delta_{max} = nFDc^\circ/i_{lim} \quad (1)$$

where i_{lim} is the limiting current density, D is the diffusion coefficient, c° is the bulk concentration of the electroactive species. F is Faraday's constant, and n is the number of electrons transferred in the electrode reaction. The thickness of this diffusion layer was fitted to the time required to reach limiting-current conditions in potential-step experiments, typically 15 s, from the Cottrell equation:

$$|i| = nFD^{1/2}c^\circ/\pi^{1/2}t^{1/2} \quad (2)$$

yielding $\delta_{max}/\mathrm{cm} = 3.9(\pi D/\mathrm{cm^2\ s^{-1}\ 1\ s})^{1/2}$. In eqn. (2) t is the time, i is the current density, and the other symbols have the same meaning as in eqn. (1). The introduction of this δ_{max} gave modelled voltammograms similar to the experimental ones, also at sweep rates of 50 mV s^{-1} and lower. In a number of the experimentally recorded voltammograms, the initial potential of the sweep was kept for several seconds before starting the actual sweep, and in some cases oxidation of the niobium-containing species in the melt took place during this time. A potential step simulation was therefore included in the computer model to calculate the changes in concentration profiles due to this oxidation. The computer models were fitted to the experimental data by introducing the following parameters: (i) a reduction mechanism including the number of electrons transferred in each step and the potentials for the reduction steps obtained from the experimental voltammograms, (ii) bulk concentrations of the electroactive species, (iii) temperature, (iv) sweep rate

and (v) time at the initial potential before starting the sweep.

The computer model calculates the concentration gradient of the electroactive species at the electrode surface multiplied by $(nFv/RT)^{1/2}$ as a function of the potential (v is the sweep rate). To fit these raw data to the voltammogram, they were simply multiplied by a factor containing information about the diffusion coefficients for the electroactive species. Calculated diffusion coefficients values were close to 3×10^{-5} cm^2 s^{-1}, a value typical for complex ions in alkali halide melts.

Results

Voltammograms and models. All potentials presented in this work are referred to the standard chlorine electrode in the CsCl–NaCl eutectic melt. Figure 1 shows a voltammogram of a CsCl–NaCl eutectic melt at 823 K containing 0.4 mol% $CsNbCl_6$ recorded with a sweep rate of 0.2 V s^{-1}. The voltammogram shows three reduction steps and five oxidation steps. The reduction steps R_1 and R_2 correspond to the oxidation steps Ox_1 and Ox_2, respectively, while the third reduction step, R_3, corresponds to the three oxidation steps Ox_3, Ox_3' and Ox_3''. The cathodic current at potentials positive of – 1 V decreased during the first hours after addition of $CsNbCl_6$. To study the electrochemistry of Nb(IV) in the melt, 0.4 mol% silver was added to the melt to reduce the Nb(V) to Nb(IV),[25] and Fig. 2 shows a voltammogram of this melt recorded with a sweep rate of 0.2 V s^{-1}. The voltammogram shows six reduction steps and six corresponding oxidation steps: R_1 corresponds to Ox_1 etc. Increasing the temperature from 823 to 963 K resulted in slightly steeper deposition peaks, but otherwise the voltammogram did not change in appearance. In Fig. 3 four voltammograms of 0.5 mol% Cs_2NbOCl_5 in the CsCl–NaCl eutectic melt at 823 K are presented. The voltammograms are recorded using a constant initial anodic po-

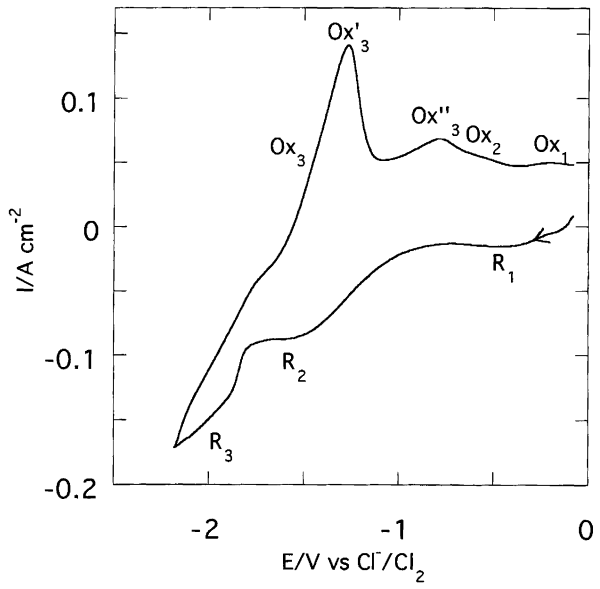

Fig. 1. Cyclic voltammogram of a CsCl–NaCl eutectic melt containing 0.4 mol% $CsNbCl_6$ at 823 K. Sweep rate 0.2 V s^{-1}.

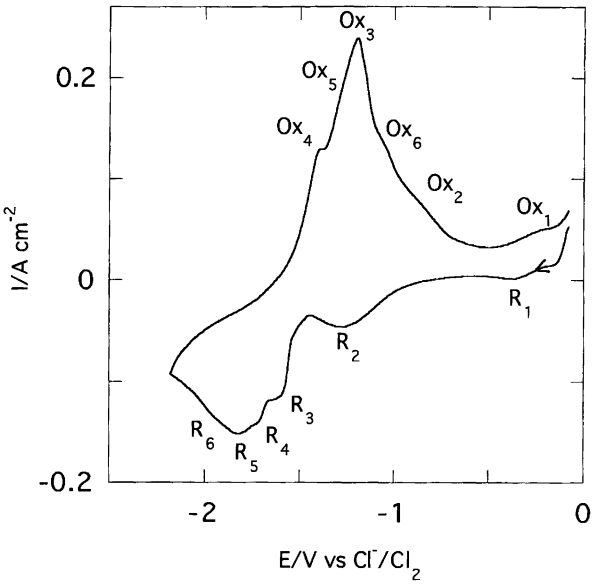

Fig. 2. Cyclic voltammogram of a CsCl–NaCl eutectic melt containing 0.4 mol% $CsNbCl_6$ and 0.4 mol Ag at 823 K. Sweep rate 0.2 V s^{-1}.

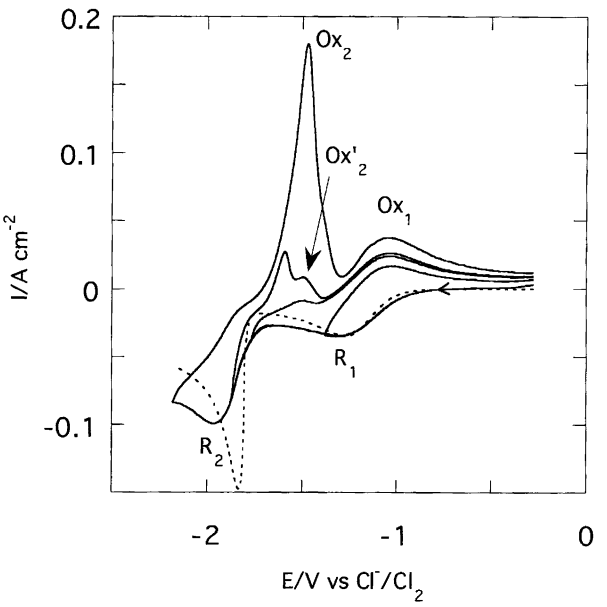

Fig. 3. Four cyclic voltammograms of a CsCl–NaCl eutectic melt containing 0.5 mol% Cs_2NbOCl_5 at 823 K. Sweep rates 0.2 V s^{-1}. An LSV model is also included in the figure. The parameters for the model were: Mechanism: $A+e^-=B$, $E^\circ = -1.19$ V, $B+2e^-=C(s)$, $E^\circ = -1.8$ V; only A is present in the bulk; temperature 823 K, sweep rate 0.2 V s^{-1}; rest time at initial potential 0 s. (——) Experimental voltammograms; (- - - -) LSV model.

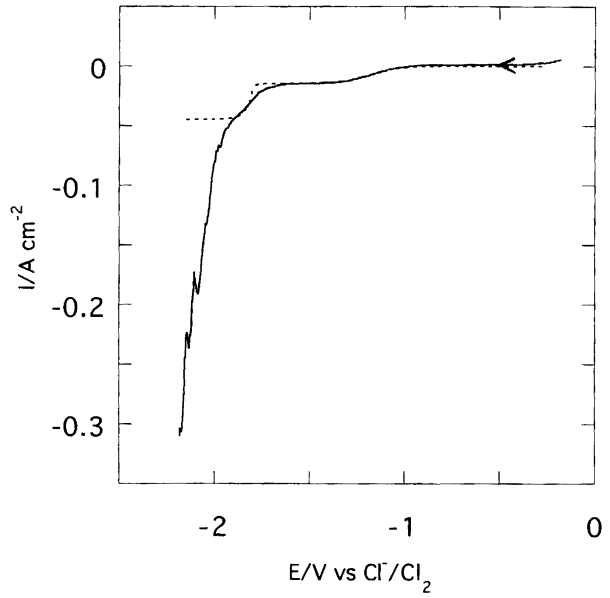

Fig. 4. Quasi-steady-state voltammogram of a CsCl–NaCl eutectic melt containing 0.5 mol% Cs_2NbOCl_5 at 823 K. Sweep rate 0.001 V s^{-1}. An LSV model is also included in the figure. The parameters for the model were: Mechanism: $A+e^-=B$, $E^\circ=-1.19$ V, $B+2e^-=C(s)$, $E^\circ=-1.8$ V; only A is present in the bulk; temperature 823 K, sweep rate 0.001 V s^{-1}, rest time at initial potential 0 s. (——) Experimental voltammogram; (- - - -) LSV model.

tential and varying the cathodic potential limit. The sweep rate was 0.2 V s^{-1}. Two reduction steps and three oxidation steps are present in the voltammogram. An LSV model is also shown. Figure 4 shows a voltammogram of the same melt as shown in Fig. 3, the sweep rate, how-

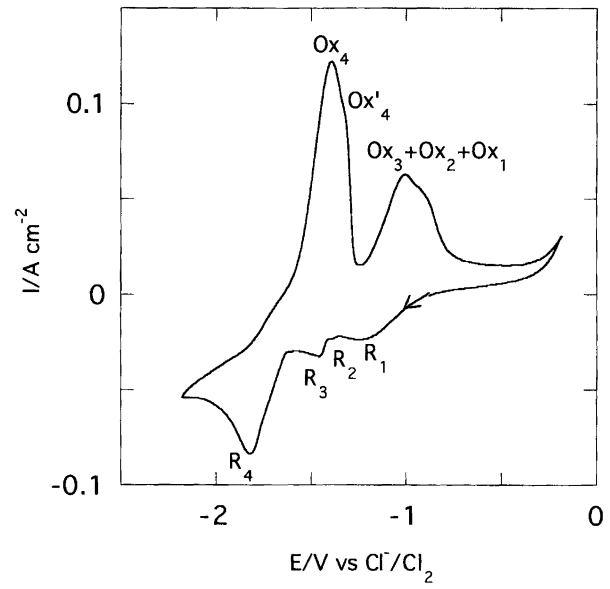

Fig. 5. Cyclic voltammogram of a CsCl–NaCl eutectic melt containing 0.5 mol% Cs_2NbOCl_5 and excess Nb_2O_5(s) at 883 K. Sweep rate 0.2 V s^{-1}.

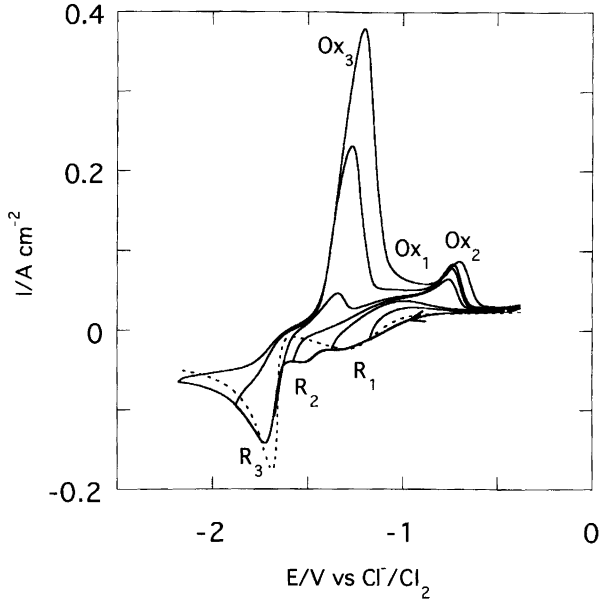

Fig. 6. Six cyclic voltammograms of a CsCl–NaCl eutectic melt containing 0.5 mol% Cs_2NbOCl_5, Nb_2O_5(s) and Nb(s) at 923 K. Sweep rates 0.2 V s^{-1}. An LSV model is also included in the figure. The parameters for the model were: Mechanism: $A+e^-=B$, $E^\circ=-1.14$ V, $B+2e^-=C(s)$, $E^\circ=-1.63$ V; only B is present in the bulk; temperature 923 K; sweep rate 0.2 V s^{-1}; rest time at initial potential 3 s. (——) Experimental voltammograms; (- - - -) LSV model.

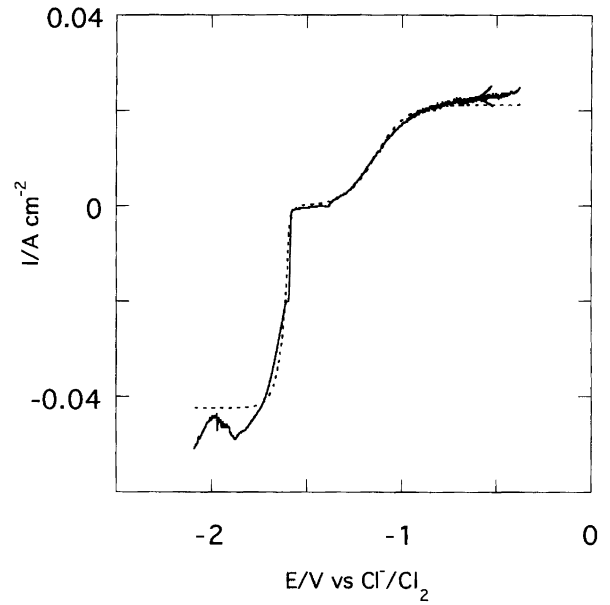

Fig. 7. Quasi-steady-state voltammogram of a CsCl–NaCl eutectic melt containing 0.5 mol% Cs_2NbOCl_5, Nb_2O_5(s) and Nb(s) at 923 K. Sweep rate 0.001 V s^{-1}. An LSV model is also included in the figure. The parameters for the model were: Mechanism: $A+e^-=B$, $E^\circ=-1.14$ V, $B+2e^-=C(s)$, $E^\circ=-1.63$ V; only B is present in the bulk; temperature 923 K, sweep rate 0.001 V s^{-1}, rest time at initial potential 3 s. (——) Experimental voltammogram; (- - - -) LSV model.

Table 2. Half-wave potentials, $E_{1/2}$, and deposition potentials for the observed reduction reactions. All potentials are referred to the standard chloride electrode.

Melt/concentrations in mol %	T/K	Red. step	$E_{1/2}$/V	E_{Dep}/V	Reduction reaction
$(CsCl–NaCl)_{eut}$+0.4% $CsNbCl_6$	823	R_1	−0.31		$NbCl_6^- + e^- = NbCl_6^{2-}$
+0.4% Ag		R_2	−1.14		$NbCl_6^{2-} + e^- = NbCl_x^{(x-3)-} + (6-x)Cl^-$
		R_3		−1.53	$Ag^+ + e^- = Ag(s)$
		R_4		−1.6	See text
		R_5		−1.8	See text
		R_6		−2.0	See text
$(CsCl–NaCl)_{eut}$+0.5% Cs_2NbOCl_5	823	R_1	−1.19		$NbOCl_5^{2-} + e^- = NbOCl_x^{(x-2)-} + (5-x)Cl^-$
		R_2		−1.8	See text
$(CsCl–NaCl)_{eut}$+0.5% Cs_2NbOCl_5	883	R_1	−1.15		$NbOCl_5^{2-} + e^- = NbOCl_x^{(x-2)-} + (5-x)Cl^-$
+Nb_2O_5(s)		R_2		−1.38	See text
		R_3		−1.43	See text
		R_4		−1.65	See text
$(CsCl–NaCl)_{eut}$+0.5% Cs_2NbOCl_5	923	R_1	−1.14		$NbOCl_5^{2-} + e^- = NbOCl_x^{(x-2)-} + (5-x)Cl^-$
+Nb_2O_5(s)+Nb(s)		R_2		−1.48	See text
		R_3		−1.60	See text

ever, being 0.001 V s^{-1}. The currents in such a voltammogram will be close to the limiting currents for all potentials, and it is therefore called a quasi-steady-state voltammogram. An LSV model is also included in this figure. To the 0.5 mol% Cs_2NbOCl_5 melt, Nb_2O_5(s) was added in excess, and in Fig. 5 a voltammogram of this melt at 883 K is shown. The voltammogram is recorded with a sweep rate of 0.2 V s^{-1} and shows four reduction steps and five oxidation steps. When the temperature was raised to 973 K, R_4 became a little steeper, and only one corresponding oxidation step was present. To the CsCl–NaCl eutectic melt containing 0.5 mol% Cs_2NbOCl_5 and an excess of Nb_2O_5(s), niobium metal was added, and six voltammograms with sweep rates of 0.2 V s^{-1} at 923 K are shown in Fig. 6. Three reduction peaks and three corresponding oxidation peaks are observed. The only change observed in the voltammograms when changing the temperature between 823 and 973 K was that R_2 became more pronounced. An LSV model is also shown in Fig. 6. Figure 7 shows an quasi-steady-state voltammogram and an LSV model of the same melt as above. A summary of the different reduction steps and the various reduction potentials is given in Table 2.

Electrodeposition experiments. Electrodeposition experiments have been performed at 823, 873, 923, 973 and 1073 K. In melts containing 1–2.5 mol% oxide-free niobium chlorides in equilibrium with Nb metal, dense and coherent niobium metal deposits were obtained at temperatures above 920 K and current densities from 15 to 100 mA cm^{-2}. At lower temperatures, however, black and incoherent non-metallic deposits were produced. Electrolysis from melts contained in platinum, glassy-carbon and fused-silica crucibles gave dense and coherent deposits when the melt was equilibrated with niobium metal. The surfaces of the dense and coherent niobium metal deposits were quite rough with varying thickness, especially for thicknesses above 0.2 mm. X-Ray analysis of the deposited metal showed only peaks belonging to niobium. The current efficiencies ranged between 30 and 60% assuming that niobium was deposited in a three-electron transfer reaction. When the dissolved niobium chlorides were not equilibrated with niobium metal, metallic deposits were obtained above 920 K, but they were powder-like and adhered poorly to the electrode. At temperatures below 920 K, black and non-metallic deposits were obtained. In a melt with O/Nb(V) = 1 at 823 K, only black, dendritic and non-metallic deposits were obtained. Similar deposits were obtained from a melt containing Nb(V) saturated with Nb_2O_5(s) at 923 K. In melts containing both Nb_2O_5(s) and Nb metal, only thin black non-metallic deposits were obtained in the temperature range 823–1023 K.

Discussion

Reduction mechanisms

Reduction mechanism of $CsNbCl_6$. The voltammogram of 0.4 mol% $CsNbCl_6$ in the CsCl–NaCl eutectic melt at 823 K (Fig. 1) shows three peaks, and the behaviour is quite different from a reversible and diffusion-controlled three-step reaction. A survey of the reduction steps is given in Table 2. Only the most anodic couple, R_1/Ox_1 with $E_{1/2} = -0.31$ V, shows reversible and diffusion-controlled behaviour. The peak current is proportional to the square root of the sweep rate, and the peak potential is independent of the sweep rate. The relation[28]

$$|E_p - E_{p/2}| = 2.2\,RT/nF \qquad (3)$$

gives n-values close to one for different sweep rates. In eqn. (3) E_p and $E_{p/2}$ are the potential at the peak and halfway up the peak, respectively, R is the gas constant,

and T, n and F have their usual meaning. Other diagnostic methods to check reversibility are difficult to apply to this reduction couple, because the standard potential for the reaction is close to the chlorine evolution potential. Because the reduction potential of Nb(V) in alkali-chloride melts is close to that of the chlorine evolution,[13] it seems reasonable to suggest that the redox couple R_1/Ox_1 is due to Nb(V)/Nb(IV). These results agree with the work of Lantelme *et al.*[15] and Picard and Bocage,[14] who found that Nb(V) is reduced reversibly and diffusion-controlled to Nb(IV) in a LiCl–KCl eutectic melt at 723 K, and that the standard potential for the reaction was −0.32 V. Elizarova *et al.*[12] and Kuznetsov *et al.*[5] reported a reduction potential of Nb(V) at ca. 0 V vs. an Ag/AgCl electrode. This is about −1.1 V referred to the standard chlorine electrode, and in view of the oxidising power of Nb(V) in alkali chloride melts,[13,25] the conclusion of these authors is probably wrong. Schäfer and Dohmann[23] observed that $NbCl_4$ disproportionates to $NbCl_5$ and $NbCl_3$ at temperatures above 573 K. However, Nb(IV) is repeatedly reported to be stable in alkali chloride melts,[2,14,15,25] indicating that $NbCl_4$ is considerably stabilised by the alkali chloride melts. Voyiatzis *et al.*[25] found that Nb(IV) is present as $NbCl_6^{2-}$ in alkali-chloride melts. The stabilising effect of the alkali-chloride melt may explain the very large difference between the observed potential for the reduction of $NbCl_6^-$ to $NbCl_6^{2-}$ in the melt and the reduction potential for reaction (1) in Table 3. The small difference in the potential between the redox couple Nb(V)/Nb(IV) and the chlorine evolution can explain the observed reduction of cathodic currents at potentials positive of −1 V in voltammograms recorded during the first hours after addition of $CsNbCl_6$. Considering the reaction

$$NbCl_6^- + Cl^- = NbCl_6^{2-} + 1/2Cl_2 \qquad (4)$$

and approximating E° with $E_{1/2}$ and using Nernst' law, we obtain

$$\frac{a_{Nb(IV)}p_{Cl_2}^{1/2}}{a_{Nb(V)}a_{Cl^-}} = \exp\frac{E_{1/2}F}{RT} = 0.015 \qquad (5)$$

where E° and $E_{1/2}$ are, respectively, the standard potential and the potential at which the concentrations of the reduced and oxidised species at the surface of the electrode are the same. At low chlorine pressures ($p_{Cl_2} \approx 2.3 \times 10^{-4}$ atm) comparable amounts of Nb(V) and Nb(IV) will exist at equilibrium. A reduction in the amount of Nb(V) will result in lower cathodic currents, as observed. The peak current for R_2 could not be evaluated, since R_2 is a shoulder on R_3. However, the anodic peak corresponding to R_2, Ox_2, has the broad shape typical of oxidation of a dissolved species, showing that the redox couple R_2/Ox_2 only involve dissolved species. When the maximum current at −1.63 V for the shoulder is plotted versus the square root of the sweep rate, a non-linear plot is obtained with decreasing slope at increasing sweep rates. Moreover, applying the reversibility condition[28]

$$|E_p^C - E_p^A| = 2.2\,RT/nF = |-1.63 - 0.83\ V| \qquad (6)$$

to R_2/Ox_2 gives $n = 0.2$. E_p^C and E_p^A are the potentials at the cathodic and anodic peak, respectively. When considering the large current value for R_2 compared to R_1, more than 0.2 electrons were obviously transferred at R_2. The second reduction step is therefore not of the reversible and diffusion-controlled type, and the number electrons transferred at R_2 can not be determined.

The third reaction step, R_3, has the characteristic shape of a deposition reaction (a sharp reduction peak and a corresponding sharp oxidation peak). The reduction step does not satisfy reversible and diffusion controlled conditions. A well defined peak did not form even when the voltammogram was swept to potentials negative of −2.18 V. However, careful examination of the voltammograms revealed that there were three oxidation steps, Ox_3, Ox_3' and Ox_3'' corresponding to R_3, of which Ox_3'' shows a quite irreversible behaviour (large potential difference between reduction and oxidation).

Reduction mechanism of $CsNbCl_6$ + Ag. When an amount of silver equal to the amount of $CsNbCl_6$ (0.4 mol%) is added to the melt, the shape of the voltammogram changes. This is seen when comparing Figs. 1 and 2. The second reduction step, R_2, changes from a shoulder to a peak, and deposition occurs at a more anodic potential. The peak potentials of steps R_1 and R_2 and the corresponding Ox_1 and Ox_2 are independent of the sweep rate, and the peak currents are proportional to the square root of the sweep rate, indicating diffusion control. Equation (3) gives one electron transferred in each step, leading to the following reduction scheme for the first two steps shown in Fig. 2; Nb(V)→Nb(IV)→Nb(III) occurring at $E_{1/2}$ values of −0.31 and −1.14 V, respectively, in good agreement with the results of Lantelme *et al.*[15] and Picard and Bocage.[14] At the potential of R_2, Elizarova *et al.*[12]

Table 3. Electrochemical reactions referred to the standard chlorine electrode at 900 K. Data from Barin.[27]

	Reaction	n	E°_{900}/V	E°_{823}/V
1	$NbCl_5(g) = NbCl_4(g) + 1/2Cl_2(g)$	1	−0.90	−0.95
2	$NbCl_4(g) = NbCl_3(s) + 1/2Cl_2(g)$	1	−0.64	−0.57
3	$NbCl_3(s) = Nb(s) + 3/2Cl_2(g)$	3	−1.30	−1.39
4	$NbO(s) + 2NaCl(l) = Nb(s) + Na_2O(s) + Cl_2(g)$	2	−3.57	−3.61
5	$2NaCl(l) + NbOCl_2(s) = Nb(s) + Na_2O(s) + 2Cl_2(g)$	4	−2.38	−2.36

Standard states: $NbCl_5(g)$, $NbCl_4(g)$, $NbCl_3(s)$, $NbOCl_2(s)$, NbO(s), Nb(s)$Na_2O(s)$, NaCl(l), all at 1 atm.

and Kutznetsov *et al.*[5] report that Nb(V) is reduced to Nb(IV). They have probably missed the first reduction step, since this is close to the chlorine evolution, and believed that the second step was the reduction of Nb(V). The observed standard potential for the reduction of Nb(IV) to Nb(III) is much more negative than the potential for reaction (2) in Table 3, and again we see that $NbCl_4$ is stabilised by the melt. Estimates for the activity coefficients for $NbCl_4$(g) and $NbCl_5$ (g and l) are given later. The equation[28]

$$|E_p - E_{p/2}| = 0.77\,RT/nF \qquad (7)$$

is valid for a reversible electrodeposition reaction. By applying this equation to R_3, $n = 1$ is obtained, and R_3 is therefore attributed to the reduction of Ag^+. Ox_3 is attributed to oxidation of silver deposited at R_3. The reduction steps R_4, R_5, R_6 and the corresponding Ox_4, Ox_5, and Ox_6 have shapes typical of deposition and stripping reactions, indicating that several deposition reactions are taking place in addition to the deposition of silver.

There are some disagreements concerning the stability of $NbCl_2$ in molten alkali chlorides.[5–11,14,15] EMF measurements,[3] together with UV–VIS–IR studies, show that Nb(III) is stable in a CsCl–NaCl eutectic containing Nb metal. A disproportionation of $NbCl_2$ to $NbCl_3$ and an insoluble species will therefore probably take place when $NbCl_2$ is added to an alkali-chloride melt.

Different reduction products of the final reduction steps of Nb(V) in alkali-chloride melts[5,8,12,15] have been proposed. The potential for the deposition reactions R_4 and R_5 compares reasonably well with the potential for reaction (3) in Table 3 when the activity of $NbCl_3$ in the melt, being ca. 0.002,[3] is taken into account. The deposition products are therefore substances with chemical potentials similar to niobium metal. Lantelme *et al.*[15] and Kuznetsov *et al.*[5] claim that the first deposition products of niobium chlorides dissolved in the LiCl–KCl eutectic at 723 K are clusters containing niobium chloride. Such clusters have a considerable degree of niobium–niobium bonds. Absorption spectroscopic investigations of the cluster compound $Na_4Nb_6Cl_{12}$ in the LiCl–KCl eutectic melt do, however, show that these clusters are unstable in melts with excess alkali chlorides and that they disproportionate to Nb(III) and a solid.[2] It therefore seems improbable that the observed non-metallic reduction products are these clusters. More likely they are subvalent alkali–niobium chlorides formed due to local supersaturation at the electrode. Alkali–niobium chloride compounds precipitated in melts with more than 0.2 mol% $NbCl_3$ when $NbCl_3$ was in equilibrium with Nb metal.[3]

Another matter of discussion is the relatively large differences in the voltammograms shown in Figs. 1 and 2. Addition of silver to the melt will reduce $NbCl_6^-$ to $NbCl_6^{2-}$ according to the reaction[25]

$$NbCl_6^- + Ag + Cl^- = NbCl_6^{2-} + AgCl. \qquad (8)$$

Adding silver to the melt should therefore give a shift of the current towards more anodic values since the bulk concentration of $NbCl_6^-$ decreases. Moreover, an extra deposition and stripping peak due to deposition and stripping of silver would be expected. These changes are observed experimentally; however, in addition to the expected changes, the current in the second reduction step decreases and R_2 takes the shape typical of a reversible and diffusion-controlled reduction. We have not been able to find a reasonable explanation for this change in the reduction mechanism. A summary of the reduction steps in the melt with $NbCl_5$ and Ag is given in Table 2.

Reduction mechanism of Cs_2NbOCl_5. When the molar ratio O/Nb is changed from zero to one, several important changes take place in the reduction mechanism, as can be seen from Fig. 3. There are no reductions taking place at potentials positive of -0.8 V in the cathodic sweep, and only two reduction peaks, R_1 and R_2, are present in the voltammogram. This observation agrees with the work of Lantelme *et al.*,[15] while Elizarova *et al.*[22] only observed one reduction peak. The oxidation peak belonging to R_1 is Ox_1 and the peaks belonging to R_2 and Ox'_2 and Ox_2. Both R_1 and R_2 show peak currents proportional to the square root of the sweep rate and peak potentials independent of the sweep rate, indicating diffusion-controlled reaction rates. Raman spectroscopic investigations[1] show that $NbOCl_5^{2-}$ is present in CsCl–NaCl eutectic melts with O/Nb = 1. Using eqn. (3) on the first reduction step gives $n \approx 1$, and it is reasonable to assume that $NbOCl_5^{2-}$ is reduced at R_1 to either a simple tetravalent niobium chloride or oxochloride. Oxide solubility measurements[29] have shown that $NbOCl_x^{(x-2)-}$ ions are stable in the CsCl–NaCl eutectic melt. It is therefore reasonable to assume that $NbOCl_5^{2-}$ is reduced to $NbOCl_x^{(x-2)-}$. The number of chlorides, x, in the Nb(IV) oxochloride is probably three, four or five. R_2 may be the sum of two reduction steps, since there is a double oxidation peak corresponding to R_2. The quasi-steady-state voltammogram in Fig. 4 supports this view, since it shows a shoulder and a sharp deposition peak at the potential of R_2. The final currents in the voltammogram in Fig. 4 are very high, and they are probably caused by an increasing area of the electrode due to dendritic growth of a conductive deposit. Deposition experiments from melts with O/Nb(V) = 1 gave black non-metallic and dendritic deposits. Electrochemical investigations show that NbO(s) is deposited on a glassy carbon electrode during electrolysis of niobium oxofluorides from a mixed chloride–fluoride melt,[19] and NbO(s) is formed in the LiCl–KCl eutectic melt when niobium oxochlorides are reduced.[14,15] The deposition product is therefore probably NbO(s), and because NbO(s) is a metallic conductor,[30] the electrode will not be passivated. However, Christensen *et al.*,[18] who studied the electrodeposition of niobium from LiF–NaF–KF eutectic melts with various O/Nb ratios, obtained metallic niobium deposits from melts with O/Nb below 0.8, and Elizarova *et al.*,[22] although presenting a reduction mechanism different from the one proposed in this work, observed niobium metal deposits at -1.8 V from a KCl–

CsCl–NaCl melt at 888 K containing $NbCl_5$ and Nb_2O_5 in a molar ratio 5/1, i.e. an O/Nb ratio equal to 0.7. Moreover, von Barner *et al.*[31] studied the reduction of $NbOF_5^{2-}$ in KCl–NaCl and found that $NbOF_5^{2-}$ was reduced to Nb(s) in a single step. Metallic niobium deposits from the melt with O/Nb = 1 would therefore not be surprising. Visual inspection of the deposit, however, showed no metal.

The LSV model data shown in Fig. 3 are in reasonable agreement with R_1, but R_2 is not as steep as predicted by the model, and the peak current is somewhat lower. The deposition reaction is therefore not completely described by a simple reduction of $NbOCl_x^{(x-2)-}$ to NbO(s), in agreement with the double oxidation peak corresponding to R_2. The LSV model shown in Fig. 4 also represents the first reduction step well, but there is a large deviation between the model and the recorded quasi-steady-state voltammogram for the deposition step. This is probably mainly due to the dendritic growth of the deposit. The reduction scheme for melts with O/Nb = 1 is given in Table 2.

Reduction mechanism of $Cs_2NbOCl_5 + Nb_2O_5$(s). In melts saturated with Nb_2O_5(s) the reduction mechanism is more complex. The voltammogram of a Nb(V) melt saturated with Nb_2O_5(s) in Fig. 5 shows two additional reduction peaks, R_2 and R_3, at − 1.38 and − 1.43 V, respectively. R_2 and R_3 were also present when a platinum working electrode was used. The currents for these peaks increased relative to R_1 with increasing temperature. The oxidation corresponding to R_2 and R_3, Ox_2 and Ox_3, takes place at a potential slightly anodic of Ox_1. R_3 has the typical shape of a deposition reaction. Solubility measurements of Nb_2O_5 in a CsCl–NaCl eutectic melt containing from 0.5 to 10 mol% $NbCl_5$ at 923 K showed that O/Nb was 1.2.[29] A melt containing Nb(V) saturated with Nb_2O_5(s) will therefore probably contain niobium oxochlorides with molar ratios O/Nb = 1 and 2. $NbO_2F_x^{(x-1)-}$ ions have been found in alkali fluoride melts[32] and in mixed alkali fluoride-chloride melts.[31] A molar ratio O/Nb = 1.2 gives a ratio $NbOCl_5^{2-}/NbO_2Cl_x^{(x-1)-} = 4$. It therefore seems reasonable to assume that $NbO_2Cl_x^{(x-1)-}$ is reduced to NbO_2(s), which deposits at R_3, and that NbO_2(s) is oxidised to $NbO_2Cl_x^{(x-1)-}$ at Ox_2. The number of chlorides, x, in $NbO_2Cl_x^{(x-1)-}$ is probably three or four. The origin for the reduction step R_2 has not been found. An increasing solubility of Nb_2O_5 with increasing temperature can explain the observed larger current for R_3 at higher temperatures. NbO_2(s) is an n-type semiconductor with electrical conductivity equal 0.01 Ω^{-1} at 823 K,[30] and will therefore not passivate the electrode. Picard and Bocage[14] claim that NbO_2(s) has a stability range of 0.25 V in the LiCl–KCl eutectic melt at 723 K, in reasonable agreement with the potential difference between R_3 and R_4 in Fig. 5. Since R_4 shows diffusion controlled behaviour, a dissolved species, probably $NbOCl_x^{(x-2)-}$, is reduced at R_4, and the reduction product is probably NbO(s), the same as for melts not saturated with Nb_2O_5. Because the oxidation step for NbO_2(s), Ox_2, was present also when sweeps to potentials cathodic of R_4 were performed, solid state reduction of NbO_2(s) to NbO(s) did not take place on the timescales studied. R_4 is shifted anodically compared to R_2 in Fig. 3, but otherwise the peaks show a similar behaviour with a corresponding double oxidation peak and a shoulder on the deposition peak appearing in quasi-steady-state voltammograms. The anodic shift of the final deposition step can be explained if a deposition overvoltage is introduced for the deposition of NbO(s) on glassy carbon. In melts saturated with Nb_2O_5(s), NbO(s) may deposit on NbO_2(s), and the deposition overvoltage on glassy carbon will disappear. However, again we emphasise that the deposition step R_4 can not be described completely by a simple reversible reduction of $NbOCl_x^{(x-2)-}$ to NbO(s). The reduction steps for niobium oxochlorides in the CsCl–NaCl eutectic melt saturated with Nb_2O_5(s) are given in Table 2.

Reduction mechanism of $Cs_2NbOCl_5 + Nb_2O_5$(s) + Nb(s). When niobium metal was added to a melt saturated with Nb_2O_5(s), the voltammogram again changed it appearance (Fig. 6). The potential was swept from − 0.38 V towards more negative potentials. Until about − 1 V, Fig. 6 shows higher anodic currents than in melts without niobium metal, indicating an oxidation reaction. It is therefore reasonable to assume that Nb(V) oxochlorides in the melt are reduced by niobium metal to niobium-containing species with valence states lower than five, and that the oxidation reaction in the first part of the sweep is due to oxidation of reduced niobium-containing species. Cathodic of − 1 V three reduction steps, R_1, R_2 and R_3, occur as the potential is swept towards more cathodic potentials. The corresponding oxidation steps are Ox_1, Ox_2 and Ox_3. R_1/Ox_1 shows reversible and diffusion-controlled behaviour, while the potential difference between R_2 and Ox_2 indicates an irreversible reaction. R_3/Ox_3 shows behaviour typical of a diffusion-controlled deposition/stripping reaction. The R_2/Ox_2 couple was also observed by Lantelme *et al.*,[15] who assigned it to the formation of niobium carbide. This is in complete agreement with our observations. In melts with niobium in valence states four or lower, the formation of niobium carbide is spontaneous, and the carbide layer is stable at potentials negative of − 0.8 V. A thin grey layer with a metallic appearance could be observed in glassy carbon crucibles that had been in contact with melts containing lower-valent niobium ions. SEM studies of the layer showed that it contained niobium. The niobium carbide formation has not been included in the LSV model, but the modelled LSV is in reasonable agreement with R_1 given in Fig. 6 and with the quasi-steady-state voltammogram shown in Fig. 7. The deposition peaks are also fairly well modelled. The model also represents well voltammograms with sweep rates 50 and 10 mV s^{-1}. The good agreement between the modelled and the experi-

mental voltammograms allows us to assume that the stable valence state of niobium oxochlorides in equilibrium with Nb metal in melts saturated with $Nb_2O_5(s)$ is four, since the model is made having only Nb(IV) in the bulk. UV–VIS–IR absorption measurements gave the same conclusion.[2] Moreover, the standard Gibbs free energy, $\Delta_r G^\circ_{900}$, for the reaction

$$2NbCl_3(s) + Nb_2O_5(s) + Nb(s) = 3NbOCl_2(s) + 2NbO(s) \quad (9)$$

is -96.5 kJ mol^{-1}, indicating that $NbCl_3(s)$ will react with $Nb_2O_5(s)$ and Nb(s) to form Nb(IV) oxochlorides and NbO(s). The final reduction steps also changed when niobium metal was added to the melt. No shoulder was present on the deposition peak, and only one corresponding oxidation step was observed, indicating a simpler deposition/stripping mechanism. However, since the shapes of the modelled and experimental deposition peaks are different, the deposition is not completely reversible. With niobium metal present, deposition experiments gave thin, smooth and black non-metallic deposits. Another interesting feature of the voltammogram in Fig. 6 is that the peak belonging to the deposition of $NbO_2(s)$ has disappeared, suggesting that niobium oxochlorides with O/Nb = 2 are no longer stable in the melt when niobium(V) in the melt is reduced to niobium(IV) by the metal. This agrees with the proposed reduction scheme for $NbO_2Cl_x^{(x-1)-}$, which when reduced, deposits as $NbO_2(s)$. $NbOCl_5^{2-}$, on the other hand, is reduced to $NbOCl_x^{(x-2)-}$, which remains dissolved in the melt. A summary of the reduction steps is given in Table 2.

Niobium deposition. Both bulk valence states and temperature are important parameters for the quality of the deposited product during electrodeposition of niobium from alkali chloride melts. To obtain dense and coherent metal deposits, equilibrium should be established between niobium metal and the dissolved niobium chlorides. Moreover, our results show that the temperature must be above about 920 K to obtain metallic niobium deposits. This agrees with the work of Lantelme *et al.*[15] and Kutznetsov *et al.*[5] They claimed that subvalent niobium compounds that deposits at temperatures below 920 K are unstable at higher temperatures. Formation of metal rather than subvalent niobium compounds is therefore favoured at temperatures above 920 K. In this work, slightly steeper deposition peaks were observed when the temperature was increased, indicating more reversible deposition reactions.

The oxide content of the melt is also important. Christensen *et al.*[18] obtained good niobium deposits in LiF–NaF–KF eutectic melts with O/Nb < 0.8, while in melts with higher O/Nb ratios partly metallic and non-metallic deposits were obtained. Elizarova *et al.*[22] also obtained niobium metal deposits from a NaCl–KCl–CsCl melt with an O/Nb ratio equal 0.7. In our deposition experiments from melts with O/Nb ≥ 1, metallic niobium deposits were not obtained. A reasonable explanation for these observations can be given if we consider the volume in the vicinity of the electrode where the reduction takes place. When the niobium oxochlorides are reduced to Nb(s), oxide ions are released and diffuse away from the electrode. This reaction will lead to relatively high concentrations of oxide ions close to the electrode. According to Picard and Bocage,[14] the reduction of NbO(s) to Nb(s) is shifted to more negative potentials with increasing oxide concentration, and at sufficiently high oxide concentrations NbO(s) can not be reduced to Nb(s) within the potential window of the solvent. The potential for reduction of NbO(s) and $NbOCl_x^{(x-2)-}$ decreases rapidly with increasing O^{2-} ion activity. This can be seen from reactions (4) and (5) in Table 3. In melts with O/Nb < 1, niobium chlorides in the vicinity of the electrode will react with the oxide ions, leading to lower oxide activities at the electrode than in melts with O/Nb ≥ 1. Thus, reduction of NbO(s) to Nb(s) can take place. The oxide activity in the melt is therefore an important parameter during electrodeposition of niobium from oxochloride melts.

Electrolysis from melts with niobium-containing ions in equilibrium with niobium metal in fused quartz crucibles gave dense and coherent niobium deposits. Raman spectroscopy has shown that $NbCl_6^-$ reacts slowly with fused silica in the CsCl–NaCl eutectic melt, and finally only the oxochloride $NbOCl_5^{2-}$ is present.[24] Niobium metal deposits were also expected from melts in equilibrium with niobium metal and $Nb_2O_5(s)$. However, no metal deposits were obtained from such melts. The difference in acid/base properties between a melt saturated with $SiO_2(s)$ and a melt saturated with $Nb_2O_5(s)$ can explain this difference. The standard Gibbs free energy at 900 K for the reaction.

$$2Nb_2O_5(s) + 5SiCl_4(g) = 5SiO_2(s) + 4NbCl_5(g) \quad (10)$$

is -158.4 kJ mol^{-1}. The oxide donor ability of $Nb_2O_5(s)$ is therefore larger than that of $SiO_2(s)$, and melts saturated with $Nb_2O_5(s)$ will have a larger oxide activity than melts saturated with $SiO_2(s)$. Because the reduction of NbO(s) to Nb metal is shifted to more negative potentials with increasing oxide activity, metal deposits are harder to obtain from melts in contact with $Nb_2O_5(s)$ than with $SiO_2(s)$.

Calculation of activity coefficients. The observed peaks in the voltammogram in Fig. 2 together with thermodynamic data allow us to estimate the activity coefficients of niobium-containing species in the melt. When the diffusion coefficients of the oxidised and reduced species are the same, the equation

$$E_{1/2} - E^\circ = -\frac{RT}{nF} \ln \frac{\gamma_{Red}}{\gamma_{Ox}} \quad (11)$$

is valid.[33] γ_{Red} and γ_{Ox} are the activity coefficients of the reduced and oxidised species, respectively. At the half-

Table 4. Activity coefficients of niobium chlorides in the CsCl–NaCl eutectic melt at 823 K and 0.4 mol%.

Species	Activity coefficients[a] (mole fraction scale)	Standard state
$NbCl_5$	0.036	$NbCl_5$(l)
$NbCl_5$	1.3	$NbCl_5$(g), 1 atm
$NbCl_4$	1.6×10^{-4}	$NbCl_4$(g), 1 atm
$NbCl_3$	0.49[b]	$NbCl_3$(s)

[a] The activity coefficients are calculated from eqn. (13) and $E_{1/2}$ for the reactions $Nb(V)+e^-=Nb(IV)$ and $Nb(IV)+e^-=Nb(III)$. [b] Ref. 3.

wave potential, $E_{1/2}$, the current is 85% of the peak current for a reversible and diffusion-controlled reaction,[33] and the concentration of the oxidised and reduced species at the electrode are theoretically the same. In the oxide-free melts, the activity coefficients of $NbCl_4$ and $NbCl_5$ with the standard states listed in Table 3 can be estimated knowing the half-wave potentials for R_1 and R_2 given in Fig. 2, the standard potentials for reactions (1) and (2) in Table 3 taken at 823 K, and the activity coefficient of $NbCl_3$. The activity coefficient of $NbCl_3$ can be calculated from thermodynamic data[3] assuming that Henry's law is valid. At 823 K and 0.2 mol% $NbCl_3$, $\gamma_{NbCl_3}=0.49$ using $NbCl_3$(s) as standard state. The activity coefficients of $NbCl_5$ and $NbCl_4$ in the eutectic containing 0.4 mol% $NbCl_5$ at 823 K obtained from eqn. (11) are given in Table 4. The relation

$$\gamma_{NbCl_5(l)} = \exp\left(\frac{\Delta_{vap}G_{823}}{RT} + \ln\gamma_{NbCl_5(g)}\right)$$

can be used to estimate the activity coefficient of $NbCl_5$ using $NbCl_5$(l) as standard state [(l) and (g) indicate liquid and gas standard states, respectively]. The Gibbs free energy of evaporation of $NbCl_5$ at 823 K, $\Delta_{vap}G_{823}$, is estimated from thermodynamic data[27] to be -24.6 kJ mol^{-1}. Activity coefficients are given in Table 4. The very low activity coefficient of $NbCl_4$ reflects the highly stability of the $NbCl_6^{2-}$ ion in the melt relative to gaseous $NbCl_4$. This means that the standard Gibbs free energy change for the reaction

$$NbCl_4(g) + 2(Na,Cs)Cl = (Na,Cs)_2NbCl_6 \quad (12)$$

is large and negative. $NbCl_5$ also shows considerable negative deviation from ideality, although not as negative as $NbCl_4$. The vapour pressure of pure $NbCl_5$ at 823 K is about 40 atm.[27] Above NbCl–CsCl mixtures the yellow colour of gaseous $NbCl_5$ can be observed,[1] but the vapour pressure are considerably lower than 40 atm. The estimated activity coefficient of $NbCl_5$ therefore seems reasonable. Since the reference pressure for the gaseous species is 1 atm, the partial vapour pressures of $NbCl_5$ and $NbCl_4$ above dilute solutions of $NbCl_5$ and $NbCl_4$ in the CsCl–NaCl eutectic melt can be estimated from the relation $P/\text{atm} = x\gamma$, indicating very low pressures of $NbCl_4$.

Conclusion

In the oxide-free CsCl–NaCl eutectic melt, reduction of Nb(V) chlorides gives Nb(IV) and Nb(III) chlorides according to the reduction reactions

$$NbCl_6^- + e^- = NbCl_6^{2-} \quad (13)$$

$$NbCl_6^{2-} + e^- = NbCl_x^{(x-3)-} + (6-x)Cl^-, \quad (x = 4, 5 \text{ or } 6) \quad (14)$$

Both reactions are reversible and diffusion-controlled. The reduction products of $NbCl_x^{(x-3)-}$ are non-metallic solids at temperatures below about 920 K and metallic niobium above this temperature.

The stable niobium oxochlorides in melts saturated with Nb_2O_5(s) are $NbOCl_5^{2-}$, $NbO_2Cl_x^{(x-1)-}$ and $NbOCl_x^{(x-2)-}$. The reduction reaction

$$NbOCl_5^{2-} + e^- = NbOCl_x^{(2-x)-} + (5-x)Cl^-, \quad (x = 3, 4 \text{ or } 5) \quad (15)$$

is reversible and diffusion-controlled. The reduction products of $NbO_2Cl_x^{(x-1)-}$ and $NbOCl_x^{(x-2)-}$ are probably NbO_2(s) and NbO(s), respectively.

To obtain dense and coherent niobium metal deposits from the CsCl–NaCl melt, the molar ratio O/Nb must be lower than one, niobium-containing ions must be in equilibrium with niobium metal, and temperatures must be higher than about 920 K.

Acknowledgements. This project has benefited scientifically from our participation in a Human Capital and Mobility Network. We appreciate interesting discussions with Prof. W. Freyland, University Karlsruhe, Germany, and Prof. G. N. Papatheodorou, University of Patras, Greece, on the structure of niobium chloride containing melts. Financial support from the Norwegian Research Council is also gratefully acknowledged.

References

1. Rosenkilde, C. and Østvold, T. *Molten Salt Forum 1-2* (1993–94) 87.
2. Bachtler, M., Rockenberger, J., Freyland, W., Rosenkilde, C. and Østvold, T. *J. Phys. Chem. 98* (1994) 742.
3. Rosenkilde, C. and Østvold, T. *Acta Chem. Scand. A 48* (1994) 732.
4. Mellors, G. W. and Senderoff, S. *J. Electrochem. Soc. 112* (1965) 266.
5. Kuznetsov, S. A., Morachevskii, A. G. and Stangrit, P. T. *Sov. Electrochem. 18* (1982) 1357.
6. Dartnell, J., Johnson, K. E. and Shreir, L. L. *J. Less Comm. Met. 6* (1964) 85.
7. Ivanovskii, L. E. and Krasil'nikov, M. T. *Electrochemistry of Molten Salts and Solid Electrolytes 4* (1967) 71.
8. Nakagawa, I. and Hirabayashi, Y. *Denki Kagaku 51* (1983) 256.
9. Vasin, B. D., Maslov, S. V., Raspopin, S. P., Kalinin, M. G. and Sukhinin, D. B. *Rasplavy 4* (1990) 48.
10. Yang, L., Hudson, R. L. and Chien, C. Y. *Met. Soc. Conf. 8* (1961) 925.

11. Suzuki, T. *Electrochim. Acta 15* (1970) 127.
12. Elizarova, I. R., Polyakov, E. G. and Polyakova, L. P. *Elektrokhimiya 27* (1991) 640.
13. Arurault, L., Bouteillon, J., de Lepinay, J., Khalidi, A. and Piognet, J. C. *Mat. Sci. Forum 73–75* (1991) 305.
14. Picard, G. and Bocage, P. *Mat. Sci. Forum 73–75* (1991) 505.
15. Lantelme, F., Barhoun, A. and Chevalet, J. *J. Electrochem. Soc. 140* (1993) 324.
16. Qiao, Z. and Taxil, P. *J. Appl. Electrochem. 15* (1985) 259.
17. Capsimalis, G. P., Chen, E. S., Peterson, R. E. and Ahmad, I. *J. Appl. Electrochem. 17* (1987) 253.
18. Christensen, E., Wang, X., von Barner, J. H., Østvold, T. and Bjerrum, N. J. *J. Electrochem. Soc. 141* (1994) 1212.
19. Chemla, M. and Grinewitch, V. *Bull. Soc. Chim. Fr.* (1973) 853.
20. Alimova, Z., Polyakov, E., Polyakova, L. and Kremenstkiy, V. *J. Fluorine Chem. 59* (1992) 203.
21. Konstantinov, V. I., Polyakov, E. G. and Stangrit, P. T. *Electrochim. Acta 26* (1981) 445.
22. Elizarova, I. R., Polyakov, E. G. and Polyakova, L. P. *Elektrokhimiya 27* (1991) 755.
23. Schäfer, H. and Dohmann, K.-D. *Z. Anorg. Allg. Chem. 300* (1959) 1.
24. Rosenkilde, C., Voyiatzis, G. A., Jensen, V. R., Ystenes, M. and Østvold, T. *Inorg. Chem. Submitted.*
25. Voyiatzis, G. A., Pavlatou, E. A., Papatheodorou, G. N., Bachtler, M. and Freyland, W. *Proc. Int. Symp. Molten Salt Chem. Techn. Electrochem. Soc. 93-9* (1993) 252.
26. Britz, D. *Digital Simulation in Electrochemistry*, Springer-Verlag, Berlin 1988.
27. Barin, I. *Thermochemical Data of Pure Substances*, VCH, Mannheim 1989.
28. Southampton Electrochemistry Group, *Instrumental Methods in Electrochemistry*, Ellis Horwood, London 1990, p. 185.
29. Rosenkilde, C. and Østvold, T. *Acta Chem. Scand. Submitted.*
30. Roberson, J. A. and Rapp, R. A. *J. Phys. Chem. Solids 30* (1969) 1119.
31. von Barner, J. H., Berg, R. W., Berghoute, Y. and Lantelme, F. *Molten Salt Forum 1-2* (1993/94) 121.
32. von Barner, J. H., Christensen, E., Bjerrum, N. J. and Gilbert, B. *Inorg. Chem. 30* (1991) 561.
33. Matsuda, H. and Ayabe, Y. *Z. Elektrochem. 59* (1955) 494.

Received June 8, 1994.